Water Science & Technology

IWA PUBLISHING

Water Science & Technology Vol 85 No 4, 1079 doi: 10.2166/wst.2022.016

Effects of electroflocculation/oxidation pretreatment on the fouling characteristics of ultrafiltration membranes

Yinghua Li*, Yiyan Wang, Mengxi Liao, Fei Su, Yue Zhang and Linlin Peng

School of Resources and Civil Engineering, Northeastern University, Shenyang, China
*Corresponding author. E-mail: liyinghua@mail.neu.edu.cn

YW, 0000-0003-3414-4187

ABSTRACT

In order to reduce the membrane pollution of ultrafiltration caused by natural organic matter and improve the treatment efficiency, electroflocculation/oxidation is used as the premembrane treatment method. The membrane specific flux attenuation characteristics was compared and analyzed under the conditions of direct ultrafiltration and electroflocculation/oxidation-ultrafiltration. Combined with the analysis of the reversibility of membrane fouling, the mechanism of electroflocculation/oxidation pretreatment to alleviate ultrafiltration membrane fouling was evaluated, and the membrane pore clogging model was used to fit the fouling law. The results show that, in the continuously fed filtration experiment, the electroflocculation/oxidation process involved in the pretreatment and the direct ultrafiltration membrane filtration decreased the ultrafiltration membrane flux to 79.1% and 28.5%, respectively. The reversible resistance generated by ultrafiltration and electroflocculation/oxidation-ultrafiltration processes accounted for 37.70% and 62.26% of their total pollution resistance, whereas the irreversible resistance generated accounted for 47.30% and 12.40%, respectively. Meanwhile, the direct correlation between the the flux dropped and complete clogging became less than that of the ultrafiltration process. The pretreatment significantly strengthened irreversible fouling resistance of the membrane pores. The membrane permeation flux was significantly increased after the electroflocculation/oxidation pretreatment.

Key words: electric flocculation/oxidation, fouling, membrane flux, pretreatment, ultrafiltration membrane

HIGHLIGHTS

- The proportion of reversible pollution via EC/O-UF dropped from 62.26% to 37.70%.
- The proportion of irreversible pollution via EC/O-UF dropped from 47.30% to 12.40%.
- With EC/O, the membrane flux increased from 28.5% to 79.1% after 3 h operation.

1. INTRODUCTION

Ultrafiltration (UF) is a high-efficiency membrane separation technology. In a pressurized environment, water flows to the other side of the UF membrane, and the pollutants are blocked and filtered. UF has advantages such as high stability, efficient separation, and high purification.

The main problem that limits the development of UF is membrane fouling. Once the membrane is contaminated, it will cause a significant decrease in the permeable flux, make the ultrafiltration process unable to operate stably for a long time, thereby affect the efficiency of ultrafiltration. At the same time, fouling significantly shortens the service life of the membrane and increases the operation costs. Therefore, how to reduce membrane pollution has become a research hotspot in this field. At present, the main measures include membrane cleaning, membrane modification, combined use of ultrafiltration and other processes, and sewage pretreatment. Chang *et al.* (2016) studied the influence of the composition of backwash water on the hydraulic cleaning performance of ultrafiltration membranes contaminated by humic acid, and found that the components of the backwash water have a significant impact on the hydraulic cleaning to alleviate membrane pollution. The increase of monovalent cations can significantly enhance the backwash efficiency, while the divalent cations can significantly reduce the efficiency. Meanwhile, the online osmotic backwash process can restore more than 90% of the membrane flux (Motsa *et al.* 2017). Although it can alleviate membrane pollution in a short period of time, improper cleaning can adversely

affect membrane performance, and improper cleaning agent selection can easily cause membrane damage. The combination of the zwitterionic structure on the poly(aryl ether oxadiazole) can effectively reduce membrane pollution and has been successfully applied to large-scale preparation of anti-fouling ultrafiltration membranes (Wang *et al.* 2021). Among them, cross-linked polyvinyl alcohol/polytetrafluoroethylene membranes showed excellent anti-fouling performance and stability under alkaline conditions (Yang *et al.* 2021). In addition, the use of hydroxyapatite-decorated activated carbon nanocomposites as membrane modifiers can improve the permeability and anti-fouling performance of ultrafiltration membranes (Parashuram *et al.* 2022). Under the coupling application conditions of UF and continuous sand filtration, polyvinylidene fluoride and polyvinyl chloride membranes can operate stably for 54 and 64 days, respectively, without any chemical cleaning (Guo *et al.* 2018; Zhang *et al.* 2022). Panitan *et al.* (2021) compared the contribution of different coagulation processes to reduce membrane pollution. The results showed that $FeCl_3$ coagulation performed better than magnetic ion exchange resin (MIEX®) and powdered activated carbon chlorination. Ultraviolet/persulfate pretreatment significantly delayed about 75% of the irreversible ultrafiltration membrane pollution caused by natural organic matter (NOM), and with the increase of persulfate dose and the extension of UV irradiation time, the fouling control performance was significantly improved (Tian *et al.* 2018). Xu *et al.* (2019) used coagulation and Fenton pretreatment processes respectively to treat the secondary effluent of recycled paper mills. Compared with direct ultrafiltration, both pretreatments can effectively alleviate membrane pollution. Shen *et al.* (2019) utilized polyaluminum chloride-polydimethyldiallyl ammonium chloride as a coagulant to pretreat wastewater before ultrafiltration, and found that flocs deposited on the membrane surface formed a loose filter cake layer, which effectively relieved membrane fouling caused by NOM.

Compared with chemical flocculant, electrocoagulation (EC) and electro-oxidation (EO) technologies have been proven to effectively remove humic acid and other dissolved organic matter with many advantages, such as less sludge, strong floc adsorption capacity, and low operating cost (Yunny *et al.* 2010; Ahmad *et al.* 2021). The filter cake layer formed by flocs protects the surface of the membrane from direct contact with pollutants and, at the same time, macromolecular organic matter is converted into low molecular weight, which can reduce membrane fouling. Therefore, this study combines the EC/O method with UF to explore the influence of electroflocculation/oxidation pretreatment on the fouling characteristics of ultrafiltration membranes. The specific goals are: (1) to analyze the influence of electroflocculation/oxidation pretreatment on membrane flux; (2) to compare the resistance distribution characteristics of membrane fouling under the conditions of direct ultrafiltration and electroflocculation/oxidation-ultrafiltration; and (3) to explore the type of ultrafiltration membrane fouling and the influence of electroflocculation/oxidation pretreatment on pollution kinetics.

2. EXPERIMENTAL MATERIALS AND METHODS

2.1. Experimental materials

2.1.1. Experimental reagents

All the experimental reagents were commercially available and analytically pure. They mainly included kaolin ($Al_2O_3 \cdot 2SiO_2 \cdot 2H_2O$), humic acid ($C_9H_9NO_6$, mass fraction 90%), fulvic acid ($C_{14}H_{12}O_8$, mass fraction 85%), sodium chloride (NaCl), sodium bicarbonate ($NaHCO_3$), sodium hydroxide (NaOH), citric acid ($C_6H_8O_7$), sodium hypochlorite (NaClO), and deionized water.

2.1.2. Experimental water

Humic acid, fulvic acid and kaolin were used to simulate NOM in water. The stock solutions were prepared by dissolving humic acid, fulvic acid and kaolin in deionized water, so that the total concentration of fulvic acid and humic acid in the NOM simulated water was 10 mg/L, and the concentration of kaolin was 50 mg/L. Among them, the mass concentration ratio of fulvic acid:humic acid in each experiment water was 2:1. The conductivity of the experimental water was 1,000 μS/cm and the pH was 7.

2.1.3. Experimental membrane

Hollow fiber polyvinylidene fluoride ultrafiltration membrane produced by Tianjin Motian Company was used, with a membrane pore size of 0.03 μm and an average molecular weight cut-off of 100,000 Daltons. Before each experiment, the membrane module is soaked in deionized water for 24 h to remove the protective agent on the membrane surface and prevent it from affecting the experiment.

2.2. Experimental device and method

2.2.1. Experimental device

As shown in Figure 1, the experimental device was composed of the ultrafiltration membrane, reaction tank, Al plate, Ti–Ru plate, electronic balance, pressure pump, pressure sensor, digital display meter, computer, and DC stabilized power supply and wires. The cross-flow filtration method was adopted. In the reaction tank, the Al and Ti–Ru plates were set as the cathode and the sacrificial anode, and an Al plate was added as the induction electrode between the two plates (the effective area of the plates was 95 cm^2 and the spacing was 25.0 mm) to form an electric flocculation/oxidation system, which was connected to a DC power supply to provide a stable voltage. During filtration, the pressure pump provides a constant transmembrane pressure (30 kPa), and the effluent is drained into a beaker set on the electronic balance. The output end of the measurement quality data of the electronic balance is connected to the computer end.

The experiment was carried out at room temperature. The current density, initial pH, and initial conductivity were maintained at 20 mA/m^2, 7, and 1,000 μS/cm, respectively. During the experiment, the water sample was filtered by the electroflocculation/oxidation-ultrafiltration system under the condition that the transmembrane pressure was 30 kPa monitored and controlled by the pressure sensor. The running duration was 3 h each time, and the changes of output were recorded during operation.

2.2.2. Analytical method

(1) Measurement of membrane flux

In the experiment, the relative flux J/J_0 is used to characterize the degree of membrane fouling under the condition of maintaining a constant transmembrane pressure difference. The readings of transmembrane pressure (TMP) and electronic scales are recorded by the pressure sensor digital display meter and data acquisition software. The membrane flux is calculated as

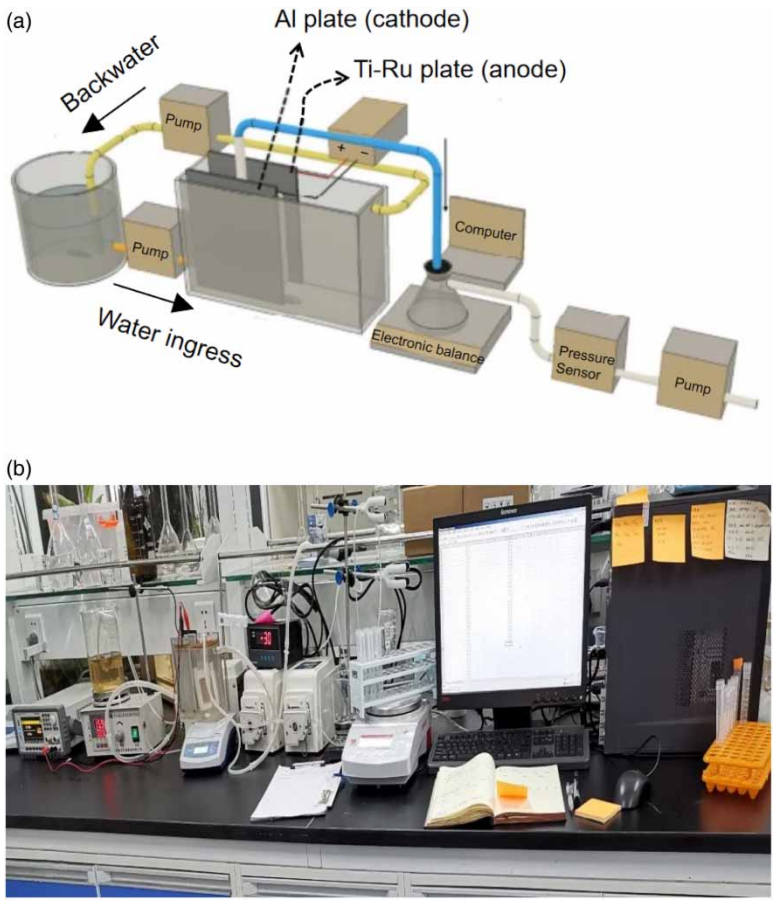

Figure 1 | The treatment process (a) and electroflocculation/oxidation-ultrafiltration device (b).

follows (Norafifah *et al.* 2015):

$$J = \frac{V}{At} \tag{1}$$

where J is the membrane permeation flux in time, $(\mathrm{L}/(\mathrm{min} \cdot \mathrm{m}^2))$; V is the volume of the permeate in time (L); t is the filtration time (min); and A is the effective area of the ultrafiltration membrane, (m^2).

(2) Measurement of membrane resistance

According to Norafifah *et al.* (2015), the total resistance of membrane fouling includes the inherent resistance of the membrane, hydraulic reversible resistance, and hydraulic irreversible resistance (Equation (2)).

$$R_t = R_m + R_r + R_{ir} \tag{2}$$

$$R_m = \frac{TMP}{J_0 \times \mu} \tag{3}$$

$$R_r = \frac{TMP}{J_1 \times \mu} - \frac{TMP}{J_2 \times \mu} \tag{4}$$

$$R_{ir} = R_t - R_m - R_r = \frac{TMP}{J_2 \times \mu} - \frac{TMP}{J_0 \times \mu} \tag{5}$$

where R_t is the total resistance of membrane fouling (m^{-1}); TMP is the transmembrane pressure (Pa); μ is the viscosity of water (Pa · s); R_m is the intrinsic membrane resistance (m^{-1}); R_r is the hydraulic reversible resistance (m^{-1}); R_{ir} is the hydraulic irreversible resistance (m^{-1}); J_0 is the pure water flux of the membrane $(\mathrm{L}/(\mathrm{m}^2 \cdot \mathrm{h}))$, J_1 is the flux when the membrane is polluted $(\mathrm{L}/(\mathrm{m}^2 \cdot \mathrm{h}))$, J_2 is the pure water flux of the membrane after backwashing $(\mathrm{L}/(\mathrm{m}^2 \cdot \mathrm{h}))$.

(3) Measurement of membrane fouling type

In the UF process, the permeation volume, filtration duration, and filtration flux data are brought into the single pollution model studied by Hermia (Lee *et al.* 2013). Since the dispersion degree of natural organic particle size of main pollutants can not be unified, a single mechanism is not convincing enough to explain the pollution phenomenon. It is considered best to use the multi-pollution combination model to analyze the pollution degree.

According to the eigenvalues of different types of blockages, a linear formula is used to simplify the Hermia model, as shown in Equations (6)–(9), and the experimental data is summarized by linear fitting of least squares.

$$\text{Filter cake clogged} \left(\frac{1}{J_0}\right) - \left(\frac{1}{J}\right) = \mathrm{D} \times V \tag{6}$$

$$\text{Completely blocked } J_0 - J = \mathrm{A} \times V \tag{7}$$

$$\text{Standard blockage } \frac{1}{\mathrm{t}} + \mathrm{B} = \frac{J_0}{V} \tag{8}$$

$$\text{Incompletely blocked } \ln J_0 - \ln J = \mathrm{C} \times V \tag{9}$$

where A, B, C, and D are constants; J is permeate flux $(\mathrm{L}/(\mathrm{m}^2 \cdot \mathrm{h}))$; and V is filtration volume (m^2).

3. RESULTS AND DISCUSSION

3.1. The influence of electroflocculation/oxidation pretreatment on membrane flux

The performance of the EC/O-UF to remove NOM depends on many factors, such as current density, floc structure, and initial conductivity (Obotey & Rathilal 2020). In order to control the experimental variables and maximize the removal efficiency by the membrane unit, according to the research of Su *et al.* (2019), the experiment was carried out at a current density of 20 $\mathrm{mA/m}^2$, initial pH of 7, and initial conductivity of 1,000 μS/cm for 3 h. The TMP was controlled at 30 kPa during the operation, and the water output of the system was monitored in real time (Figure 2).

After 3 h of continuous filtration experiment, the flux of ultrafiltration membrane in the EC/O-UF and direct UF processes dropped to 28.5% and 79.1%, respectively. In the initial stage of the experiment, membrane flux using UF alone decreased

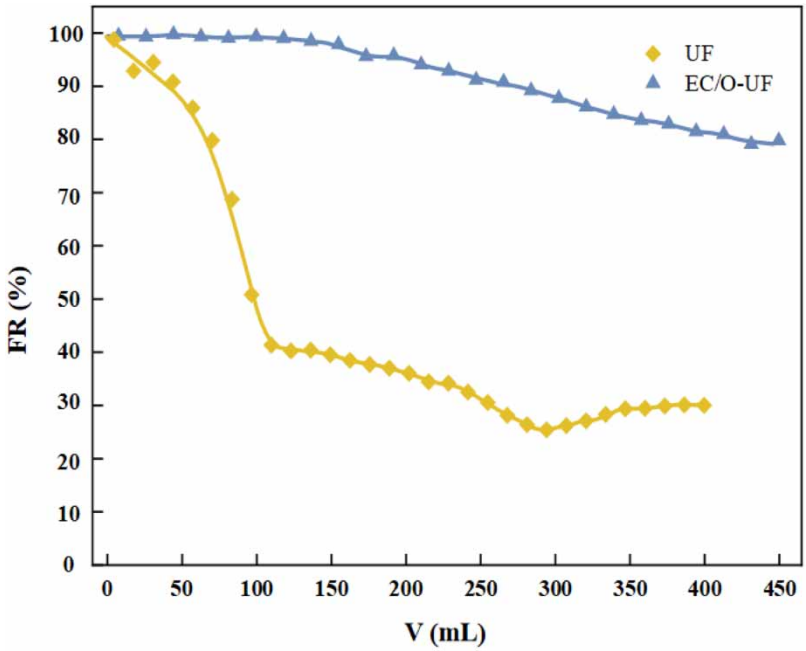

Figure 2 | Membrane flux attenuation in direct UF and EC/O-UF (FR is membrane flux recovery rate, %).

extremely rapidly and significantly. Due to the serious clogging of the membrane filaments, it remained at a low value (25.3%) in the end. By contrast, the positive effect of electroflocculation/oxidation on flux attenuation was significant. Not only the membrane attenuation pressure on the attenuation rate was alleviated, but the final membrane permeation flux also achieved a more satisfactory effect.

The most significant decline indicated that direct UF membrane pollution was serious, resulting from the accumulation of NOM on the membrane surface or membrane pores, and then the formation of a pollution layer on the membrane surface (Tahreen & Jami 2021). Compared with the use of UF alone, electroflocculation/oxidation pretreatment had a significant mitigation effect on the attenuation of the specific flux of the ultrafiltration membrane (Zazouli & Kalankesh 2017; Sardari *et al.* 2018; Du *et al.* 2019). This difference can be attributed to three aspects. First, the electrolytic oxidation of the sacrificial Ti–Ru anode produced a large number of positively charged titanium salt ions, and the negatively charged pollutants (such as humic acid) were neutralized by charge neutralization (Yin *et al.* 2020), thereby reducing the accumulation of pollutants on the membrane surface during the membrane filtration process. Secondly, the negative charge that migrated to the anode surface due to electrophoresis contaminated the colloid, forcing the chemical coagulation process between the particles and the metal hydroxide to occur near the anode, rather than at the UF membrane module. At the same time, the generated electrolytic hydrogen bubbles at the cathode made part of the flocs float (Li *et al.* 2019a, 2019b). Therefore, less pollutants accumulate or deposit on the surface of the membrane. In addition, at higher current density, more complex titanium salt–humus organic flocs were produced. Under the action of an electric field, as the solid titanium salt flocs were deposited on the surface of the membrane, a relatively loose filter cake layer was formed (Gonzalez-olmos *et al.* 2018). The filter cake layer with low hydraulic resistance reduced pollution by preventing smaller particles from reaching the membrane surface and pores and prevented the membrane pores from clogging.

The difference in flux reduction between the single UF operation and the electroflocculation/oxidation-ultrafiltration experiment indicated that the EC/O pretreatment can effectively slow down the general attenuation of flux caused by UF membrane in the process of removing NOM (Figure 3).

3.2. The influence of EC/O pretreatment on the resistance distribution of membrane fouling

Figure 4 shows the distribution of membrane resistance in the UF process of the two processes. After the filtering experiments with NOM solution simulated by humic acid, R_r generated by UF and EC/O-UF were 10.905×10^{11} m^{-1} and 10.754×10^{11} m^{-1}, respectively, accounting for 37.70% and 62.26% of their total pollution resistance R_r. Correspondingly,

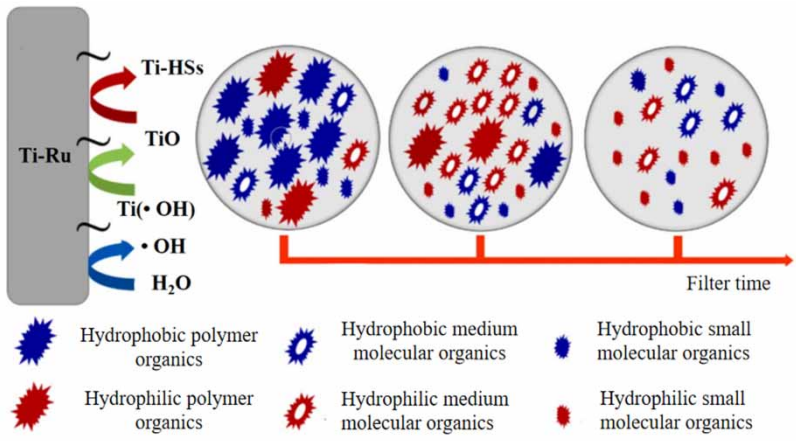

Figure 3 | Mechanism of electroflocculation/oxidation pretreatment to alleviate membrane fouling.

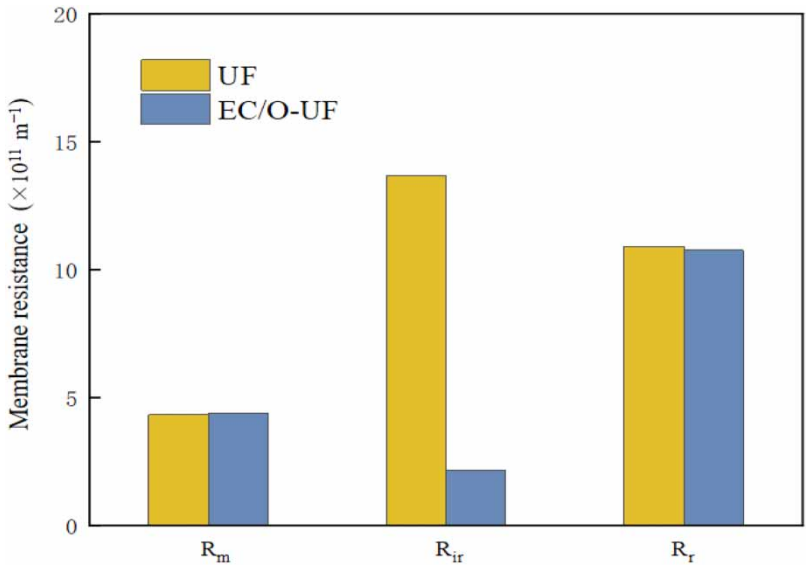

Figure 4 | Membrane resistance distribution in direct ultrafiltration and electroflocculation/oxidation-ultrafiltration processes.

R_{ir} generated were 13.681×10^{11} m^{-1} and 2.142×10^{11} m^{-1} for UF and EC/O-UF, respectively, and accounted for 47.30% and 12.40% of their total dirt resistance.

For the transmembrane resistance formed by the NOM solution on the membrane surface, the pretreatment significantly reduced the total resistance R_r. At the same time, the reversible resistance accounted more of the total resistance compared to the direct UF operation. More surface dirt can be removed directly after oxidation treatment, which undoubtedly increased the usable frequency of the membrane and produced certain economic benefits.

The macromolecule organic pollutants will be degraded into small ones after electro-oxidation (Wu *et al.* 2021), which alleviated the pollution of the filter cake layer accumulated in the membrane pores. By contrast, the reversible and irreversible fouling resistance after EC/O pretreatment was significantly alleviated, which showed that pretreatment conrolled membrane fouling caused by humic acid, especially the resistance to irreversible pollution on the membrane (Li *et al.* 2019a, 2019b). Since backwashing or other physical cleaning methods can easily reduce the reversible membrane fouling (Gul *et al.* 2021), the pretreatment had important practical significance in the application of ultrafiltration.

3.3. Effect of EC/O pretreatment on membrane pollution type

3.3.1. Fitting of combined pollution model

In order to understand the pollution mitigation mechanism of related membrane pollution through EC/O pretreatment, the combined pollution model was used to perform a nonlinear fitting between the filtration volume (V) and the filtration time (T) in Table 1.

The components of NOM that are significantly larger than the pore size of the ultrafiltration membrane (mainly suspended particles and some large-size colloids) can form fouling of the filter cake layer, while the components equivalent to the pore size of the ultrafiltration membrane (mainly colloids) can form complete and incomplete blockage. In comparison, the components significantly smaller than the pore size of the ultrafiltration membrane (mainly soluble substances and some small colloids) can form standard clogging (Iritani *et al.* 2015; Hou *et al.* 2017).

In the nonlinear fitting results, the standard clogging-filter cake clogging model of the EC/O-UF process did not converge. The combined models of complete clogging with standard clogging (R^2 0.91146), complete clogging with filter cake clogging (R^2 0.95368), and incomplete clogging with filter cake clogging (R^2 0.85747) did not pass the parameter t test. Only the combination model of incomplete clogging and standard clogging fitted better (R^2 0.98548, $t < 0.01$), as shown in Figure 5.

Since the combined model is derived from two single pollution models, the fitting parameters can be used to quantitatively evaluate the contribution of a single model. According to the definition of the fouling model, the fouling of the filter cake layer increases the filtration resistance (Racar *et al.* 2017) and causes the flux to decrease $\Delta J/J_0 = K_c J_0 V/1 + K_c J_0 V \approx K_c J_0 V$ (V is small enough). When complete clogging occurs, the clogged membrane pores lose the filtering ability, resulting in a decrease in flux $\Delta J/J_0 = (K_b/J_0)V$. Therefore, the ratio $\Delta J/J_0$ and $K_c J_0/(K_b/J_0)$ of the above two specific fluxes can be used to quantitatively evaluate the contribution of the filter cake layer and complete blockage pollution to the decrease of membrane flux.

The $K_c J_0/(K_b/J_0)$ values of UF and EC/O-UF were 0.0686 and 0.0408, respectively (that is, the fouling rate of complete blockage with reduced flux were 94.26% and 85.56%, respectively), it shows that complete fouling was decisive for the decrease of the ultrafiltration membrane flux in this study. Once the complete clogging occurs, the clogged membrane pores lost the filtering capacity (that is, the resistance was infinite), and the resistance caused by the contamination of the filter cake layer was limited. Therefore, the flux attenuation caused by complete blockage was greater than that caused by the filter cake layer formed by suspended particles (Ren *et al.* 2021).

The K_c and K_b of UF were higher than those of EC/O-UF, which may be related to the influent quality, where K_c is the area of pollution layer formed by unit flux for filter cake clogging and K_b is the area of pollution layer formed by unit flux for complete clogging. The concentration of suspended particles and organic colloids (turbidity) in the filtrate without electroflocculation/oxidation pretreatment was higher. However, if the particle size of the suspended particles was greater

Table 1 | Fitting situation table of direct UF and EC/O-UF membrane fouling model

	Without pretreatment		Electric flocculation/oxidation pretreatment	
Model	**R^2**	**Characteristic parameters**	**R^2**	**Characteristic parameters**
Completely blocked–standard blocked	0.94852	$K_b = 2.79 \times 10^{-5}\ s^{-1}$ $K_s = 8.63\ m^{-1}$	0.91146	$K_b = 4.95 \times 10^{-6}\ s^{-1}$ $K_s = 11.14\ m^{-1}$
Completely blocked–standard blocked	0.97295	$K_c = 5.81 \times 10^{4}\ s/m^2$ $K_s = 8.85\ m^{-1}$	0.95368	$K_c = 0.74 \times 10^{4}\ s/m^2$ $K_s = 3.99\ m^{-1}$
Incomplete clogging–filter cake clogging	0.68932	$K_c = 2.02 \times 10^{4}\ s/m^2$ $K_i = 71.18\ m^{-1}$	0.85747	$K_c = 1.35 \times 10^{4}\ s/m^2$ $K_i = 43.38\ m^{-1}$
Incomplete clogging–filter cake clogging	0.76075	$K_i = 5.05\ m^{-1}$ $K_s = 1.66\ m^{-1}$	0.98548	$K_i = 5.05\ m^{-1}$ $K_s = 8.37\ m^{-1}$
Standard clogging–filter cake clogging	No fit trend	– –	No fit trend	– –
Completely blocked	0.96584	$K_b = 1.95 \times 10^{-4}\ s^{-1}$	0.82745	$K_b = 0.94 \times 10^{-5}\ s^{-1}$
Standard blockage	0.91496	$K_s = 4.28\ m^{-1}$	0.97295	$K_s = 3.28\ m^{-1}$
Filter cake clogged	0.74034	$K_c = 2.09 \times 10^{4}\ s/m^2$	0.85397	$K_c = 0.60 \times 10^{4}\ s/m^2$
Not completely blocked	0.85134	$K_i = 9.22\ m^{-1}$	0.81632	$K_i = 5.31\ m^{-1}$

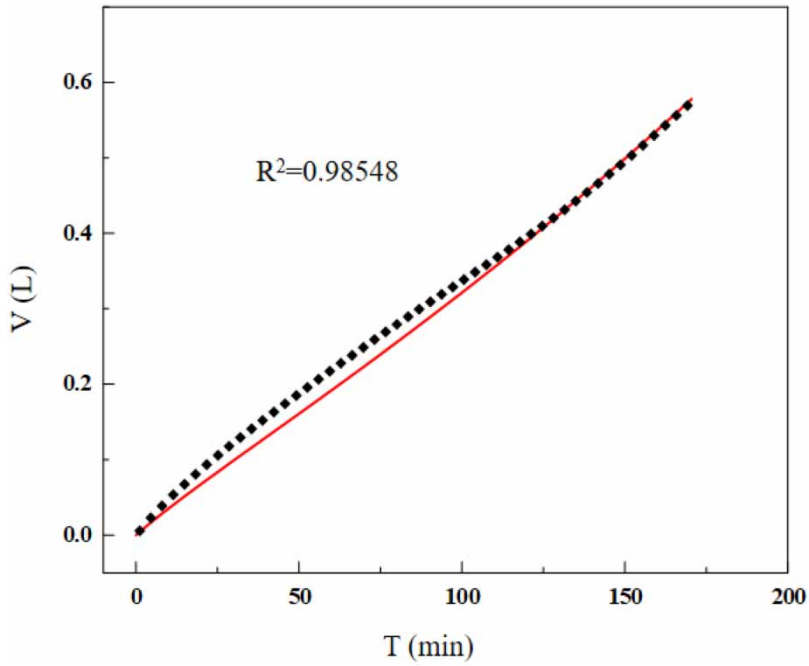

Figure 5 | Fitting of incomplete clogging-standard clogging model of EC/O-UF.

than 0.45 μm, the filter cake layer will be blocked, and the organic colloid with the same or similar molecular weight cut-off value (150 kda) of the ultrafiltration membrane can form a complete blockage.

The $K_cJ_0/(K_b/J_0)$ value of direct UF was lower than that of EC/O-UF, indicating that the direct correlation between complete clogging and the flux drop in the EC/O-UF process was less. It reflected the performance of electroflocculation/oxidation pretreatment to remove suspended particles.

3.3.2. Fitting of single pollution model

By fitting the Hermia models for UF and EC/O-UF, the results are shown in Figure 6. Referring to Figure 6(a), it can be seen that the correlation coefficient R^2 of complete blockage model was higher than those of the other models, indicating that the complete clogging was the main reason of membrane pollution for UF process. Referring to Figure 6(g), in the performance of EC/O-UF, the filter cake clogging model had a better linear fit with R^2 of 0.97295. This also confirmed the results obtained by fitting the combined pollution model, showing that the electroflocculation/oxidation pretreatment can reduce the complete clogging and increase the membrane permeation flux (Xiong *et al.* 2016).

When the cross-flow velocity was stable, the contaminants will separate from the membrane surface and return to the filter solution, so the filter cake layer will stop growing, the filter cake filtering mechanism is replaced by standard clogging, and the main fouling mechanism is converted to standard clogging. Due to the electrostatic repulsion between the membrane surfaces and the reduction of contaminants, low molecular weight substances had stronger adhesion in the membrane pores, which was related to the standard blocking mechanism.

4. CONCLUSIONS

Membrane fouling can cause significant decrease in the permeable flux, treatment efficiency, and the service life of the membrane. In this study, the mitigation effect of electroflocculation/oxidation as membrane pretreatment on ultrafiltration membrane pollution caused by NOM were quantitatively studied by measuring membrane flux, calculating membrane resistance, and discussing the types of membrane pollution. The main findings are as follows:

(1) Compared with ultrafiltration, electroflocculation/oxidation-ultrafiltration had a more significant inhibitory effect on flux attenuation.

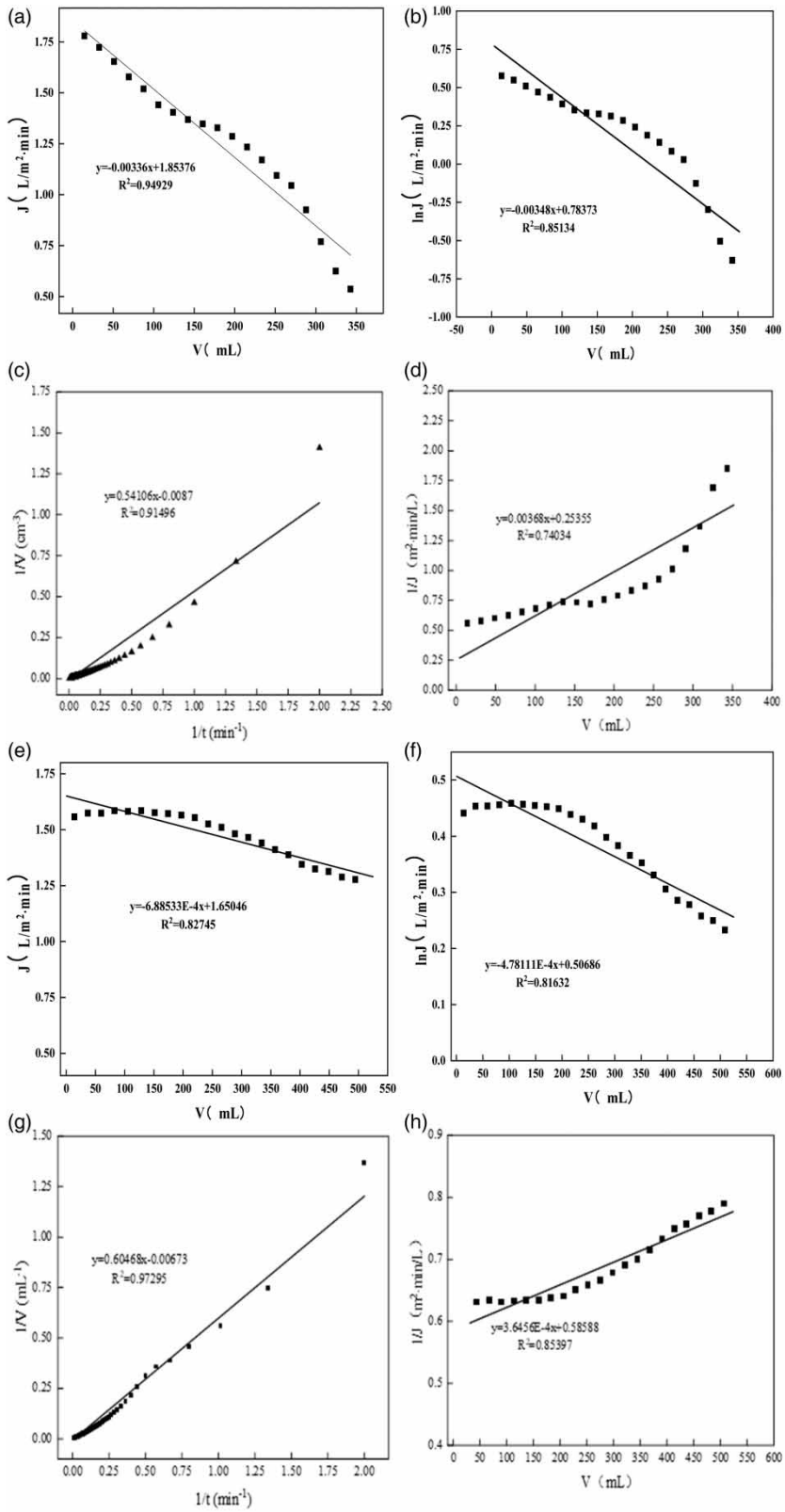

Figure 6 | Fitting results of UF and EC/O-UF. (a) UF complete clogging fitting; (b) UF incomplete clogging fitting; (c) UF filter cake clogging fitting; (d) UF standard clogging fitting; (e) EC/O-UF complete clogging fitting; (f) EC/O-UF incomplete clogging fitting; (g) EC/O-UF filter cake clogging fitting; and (h) EC/O-UF standard clogging fitting.

(2) After electroflocculation/oxidation pretreatment, both the reversible and irreversible fouling on the membrane surface had been significantly alleviated, especially the irreversible fouling.
(3) Compared with direct ultrafiltration, electroflocculation/oxidation pretreatment can significantly reduce the complete clogging risk and increase the membrane flux of ultrafiltration.

ACKNOWLEDGEMENTS

This research is supported by the National Key R&D Program of China (2019YFC1803802).

DATA AVAILABILITY STATEMENT

All relevant data are included in the paper or its Supplementary Information.

REFERENCES

Ahmad, M. S., Ab, R. M. H., Alqahtani, T. M., Witoon, T., Lim, J. W. & Cheng, C. K. 2021 A review on advances in green treatment of glycerol waste with a focus on electro-oxidation pathway. *Chemosphere* **276**, 130128.

Chang, H. Q., Liang, H., Qu, F. S., Ma, J., Ren, N. Q. & Li, G. B. 2016 Towards a better hydraulic cleaning strategy for ultrafiltration membrane fouling by humic acid: effect of backwash water composition. *Journal of Environmental Sciences* **43** (5), 177–186.

Du, X., Yang, W. P., Zhao, J., Zhang, W. X., Cheng, X. X., Liu, J. X., Wang, Z. H., Li, G. B. & Liang, H. 2019 Peroxymonosulfate-assisted electrolytic oxidation/coagulation combined with ceramic ultrafiltration for surface water treatment: membrane fouling and sulfamethazine degradation. *Membrane Fouling and Sulfamethazine Degradation* **235**, 779–788.

Gonzalez-olmos, R., Penadés, A. & Garcia, G. 2018 Electro-oxidation as efficient pretreatment to minimize the membrane fouling in water reuse processes. *Journal of Membrane Science* **552**, 124–131.

Gul, A., Hruza, J. & Yalcinkaya, F. 2021 Fouling and chemical cleaning of microfiltration membranes: a mini-review. *Polymers* **13** (6), 846–871.

Guo, Y. Q., Bai, L. M., Tang, X. B., Huang, Q. J., Xie, B. H., Wang, T. Y., Wang, J. L., Li, G. B. & Liang, H. 2018 Coupling continuous sand filtration to ultrafiltration for drinking water treatment: improved performance and membrane fouling control. *Journal of Membrane Science* **567**, 18–27.

Hou, L., Wang, Z. & Song, P. 2017 A precise combined complete blocking and cake filtration model for describing the flux variation in membrane filtration process with BSA solution. *Journal of Membrane Science* **542**, 186–194.

Iritani, I., Katagiri, N., Takenaka, T. & Yamashita, Y. 2015 Membrane pore blocking during cake formation in constant pressure and constant flux dead-end microfiltration of very dilute colloids. *Chemical Engineering Science* **122**, 465–473.

Lee, J. S., Dilaver, M., Park, P. K. & Kim, J. H. 2013 Comparative analysis of fouling characteristics of ceramic and polymeric microfiltration membranes using filtration models. *Journal of Membrane Science* **432**, 97–105.

Li, K., Li, S., Huang, T. L., Dong, C. Z., Li, J. W., Zhao, B. & Zhang, S. J. 2019a Chemical cleaning of ultrafiltration membrane fouled by humic substances: comparison between hydrogen peroxide and sodium hypochlorite. *International Journal of Environmental Research and Public Health* **16** (14), 2568.

Li, W., Su, X., Palazzolo, A. & Ahmed, S. 2019b Numerical modeling of concentration polarization and inorganic fouling growth in the pressure-driven membrane filtration process. *Journal of Membrane Science* **569**, 71–82, 130284.

Motsa, M. M., Mamba, B. B., Thwala, J. M. & Verliefde, A. R. D. 2017 Osmotic backwash of fouled FO membranes: cleaning mechanisms and membrane surface properties after cleaning. *Desalination* **402**, 62–71.

Norafifah, H., Noordin, M. Y., Wong, K. Y., Izman, S. & Aizat, A. A. N. 2015 A study of operational factors for reducing the fouling of hollow fiber membranes during wastewater filtration. *Procedia Cirp* **26**, 781–785.

Obotey, E. E. & Rathilal, S. 2020 Membrane technologies in wastewater treatment: a review. *Membranes* **10** (5), 89–117.

Panitan, J., Rose, M. C., Philip, C. S. & Orlando, C. 2021 Efficacy of selected pretreatment processes in the mitigation of low-pressure membrane fouling and its correlation to their removal of microbial DOM. *Chemosphere* **277**, 130284.

Parashuram, K., Mariam, O., Bharath, G., Shadi, H. W. & Fawzi, B. 2022 Enhanced water permeability and fouling resistance properties of ultrafiltration membranes incorporated with hydroxyapatite decorated orange-peel-derived activated carbon nanocomposites. *Chemosphere* **286**, 131799.

Racar, M., Dolar, D. & Košutić, K. 2017 Chemical cleaning of flat sheet ultrafiltration membranes fouled by effluent organic matter. *Separation and Purification Technology* **188**, 140–146.

Ren, L. M., Yu, S. L., Yang, H. J., Li, L., Cai, L. Y., Xia, Q., Shi, Z. Y. & Liu, G. C. 2021 Chemical cleaning reagent of sodium hypochlorite eroding polyvinylidene fluoride ultrafiltration membranes: aging pathway, performance decay and molecular mechanism. *Journal of Membrane Science* **625**, 119141.

Sardari, K., Peter Fyfe, P., Lincicome, D. & Ranil, S. W. 2018 Combined electrocoagulation and membrane distillation for treating high salinity produced waters. *Journal of Membrane Science* **564**, 82–96.

Shen, X., Gao, B. Y., Guo, K. Y., Yu, C. H. & Yue, Q. Y. 2019 PAC-PDMDAAC pretreatment of typical natural organic matter mixtures: ultrafiltration membrane fouling control and mechanisms. *The Science of the Total Environment* **694**, 133816.

Su, F., Li, Y. H., Deng, W. H., Li, H. B., Yang, L. & Chen, T. Y. 2019 Study on mitigating membrane fouling based on precursor and flocculant Al_b matching in EC/O-UF system. *Water Science and Technology: A Journal of the International Association on Water Pollution Research* **80**, 9.

Tahreen, A. & Jami, M. S. 2021 Advances in antifouling strategies in membrane ultrafiltration: a brief review. *Journal of Advanced Research in Materials Science* **76**, 10–16.

Tian, J. Y., Wu, C. W., Yu, H. R., Gao, S. S., Li, G. B., Cui, F. Y. & Qu, F. S. 2018 Applying ultraviolet/persulfate (UV/PS) pre-oxidation for controlling ultrafiltration membrane fouling by natural organic matter (NOM) in surface water. *Water Research* **132**, 190–199.

Wang, Z. F., Sun, N., Ma, X., Gu, J. Y., Huo, P. F., Liu, Y. & Liu, C. W. 2021 Synthesis and characterization of novel zwitterionic poly(aryl ether oxadiazole) for antifouling ultrafiltration membrane. *Journal of Environmental Chemical Engineering* **9** (5), 106206.

Wu, Y. H., Tong, X., Zhao, X. H., Bai, Y., Ikuno, N., Ishii, K. & Hu, H. Y. 2021 The molecular structures of polysaccharides affect their reverse osmosis membrane fouling behaviors. *Journal of Membrane Science* **625**, 118984.

Xiong, J. L., Fu, D. F., Singh, R. P. & Ducoste, J. J. 2016 Structural characteristics and development of the cake layer in a dynamic membrane bioreactor. *Separation and Purification Technology* **167**, 88–96.

Xu, Y. M., Li, Y. M. & Hou, Y. 2019 Reducing ultrafiltration membrane fouling during recycled paper mill wastewater treatment using pretreatment technologies: a comparison between coagulation and Fenton. *Journal of Chemical Technology & Biotechnology* **94** (3), 804–811.

Yang, K., Wang, C. F., Chen, Y. B., Xu, J. P., Sun, L. & Liu, S. R. 2021 Separation and recovery of alkali cellulose wastewater with high concentration of salts by cross-linked poly(vinyl alcohol)/polytetrafluoroethylene ultrafiltration membrane. *Journal of Water Process Engineering* **43**, 102238.

Yin, Z., Yeow, R. Q. J., Ma, Y. Q. & Chew, J. W. 2020 Link between interfacial interaction and membrane fouling during organic solvent ultrafiltration of colloidal foulants. *Journal of Membrane Science* **611**, 118369.

Yunny, M., José, A. R., Mario, A. V. & Thomas, W. C. 2010 Industrial wastewaters treated by electrocoagulation. *Electrochimica Acta* **55** (27), 8165–8171.

Zazouli, M. A. & Kalankesh, L. R. 2017 Removal of precursors and disinfection by-products (dbps) by membrane filtration from water; a review. *Journal of Environmental Health Science and Engineering* **15** (1), 1–10.

Zhang, H. R., Zhang, J. X., Luo, J. Q. & Wan, Y. H. 2022 A novel paradigm of photocatalytic cleaning for membrane fouling removal. *Journal of Membrane Science* **641**, 119859.

First received 21 October 2021; accepted in revised form 9 January 2022. Available online 21 January 2022